Anticancer effects of monocarbonyl analogs of curcumin: oxidative stress, nuclear translocation and modulation of AP-1 and NF-κB

Brian K Adams[1,2], Marike Herold[3], Eva M Ferstl[3], Jungwhan John Choi[3], Shijun Zhu[2],
Vladimir Y Bogdanov[4], Bassel F El-Rayes[2], Aiming Sun[3], Dennis C Liotta[3],
James P Snyder[3], Mamoru Shoji[2*]

[1]*Program in Molecular and Systems Pharmacology, Emory University, Atlanta, Georgia, USA*
[2]*Department of Medical Oncology, Winship Cancer Institute, Emory University, Atlanta, Georgia, USA*
[3]*Department of Chemistry, Emory University, Atlanta, Georgia, USA*
[4]*Division of Hematology/Oncology, Internal Medicine, University of Cincinnati College of Medicine, Cincinnati, Ohio, USA*

Original Article

Abstract

Purpose: In order to elucidate anticancer effects of monocarbonyl analogs of curcumin (MACs), we have undertaken the present study to obtain information regarding drug targets by using a microarray approach, and to study the cellular localization of EF24 and the activity of two key transcription factors, AP-1 and NF-κB, involved in complex cellular responses of cell survival and death. **Methods:** Cytotoxic activity of various drugs was evaluated using a Neutral Red Dye assay. Cellular localization of biotinylated EF24 (active) and reduced EF24 (inactive) was determined using light and confocal microscopy. Measurement of transcription factor binding was carried out using Transfactor ELISA kits (BD Clontech, Palo Alto, CA). Gene microarray processing was performed at Expression Analysis, Inc (Durham, NC) using Affymetrix Human U133A Gene Chips. **Results:** In this study, we demonstrated that EF24 and UBS109 exhibit much more potent cytotoxic activity against pancreatic cancer than the current standard chemotherapeutic agent gemcitabine. EF24, rapidly localizes to the cell nucleus. The compound modulates the DNA binding activity of NF-κB and AP-1 in MDA-MB-231 human breast cancer cells and DU-145 human prostate cancer cells. Immunohistochemical studies utilizing biotinylated-EF24 and chemically-reduced EF24 show that the unsaturated compound and biotinylated EF24, but not reduced EF24, translocates to the nucleus within 30 minutes after the addition of drug. Through a gene microarray study, EF24 is shown to affect genes directly involved in cytoprotection, tumor growth, angiogenesis, metastasis and apoptosis. **Conclusion:** EF24 and UBS109 warrant further investigation for development of pancreatic cancer therapy. The dualistic modulations of gene expression may be a manifestation of the cell responses for survival against oxidative stress by EF24. However, the cytotoxic action of EF24 ultimately prevails to kill the cells.

Keywords: Curcumin Analogs; EF24; UBS109; Pancreatic, Breast and Prostate Cancers; Oxidative Stress; Nuclear Translocation; NF-κB; AP-1

Introduction

Curcumin (diferuloylmethane, **Figure 1**) a major component of turmeric, is used as a coloring and flavoring agent in many food items including curries and mustards. Although curcumin has traditionally been used in Indian folk medicine for a wide range of ailments, recent pre-clinical and clinical studies demonstrate that this phytochemical also exhibits an array of anticancer properties.[1] The pharmacological safety of curcumin has been demonstrated by its consumption for centuries at average human levels of 100-200 mg/day to as high as 12 g/day in toxicity studies.[2] One potential problem with the clinical use of curcumin is its low potency, poor absorption and limited stability [3, 4]; however, curcumin remains an ideal lead compound for the design of more effective analogs.[5]

A recent review has examined the anticancer and anti-inflammatory actions of a wide range of monocarbonyl analogs of curcumin (MACs).[5] We have found that four MACs with a common mechanism of action, including EF24, EF25, EF31 and UBS109, may be clinically useful.[6-12]
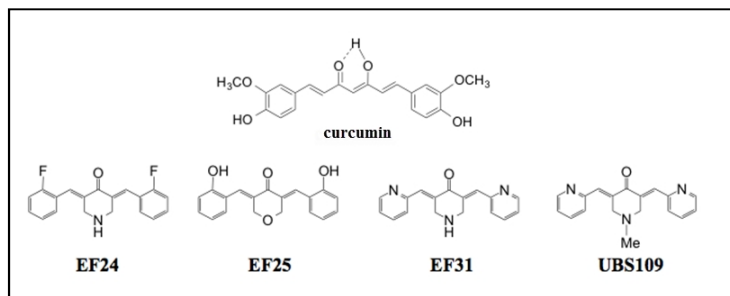
FIG. 1: Chemical structures of curcumin and analogs (MACs).

Here, we summarize tumorigenic actions of the subset of MACs considered in this work. EF24, EF25, EF31 and UBS109 inhibit a wide variety of cancer cells.[6-8, 10, 13-16] MACs also mediate inflammation [9], disrupt the microtubule cytoskeleton and inhibit HIF-1 [17], in contrast to paclitaxel, which involves stabilization of cellular microtubules, thereby interfering with normal microtubule dynamics during cell division. Tissue factor (TF) is aberrantly expressed in cancer and its vasculature and causes thrombo-embolic complications. As a complement to direct administration of the MAC molecules, we have developed a method to specifically deliver EF24 and paclitaxel to TF-expressing tumor endothelia and breast cancer cells in subcutaneous and lung metastasis models by conjugating the drugs to factor VIIa. The drug conjugates complex with TF at the cell surface followed by endocytosis of the protein aggregate and cleavage of the drugs in the cytoplasm.[18-22]
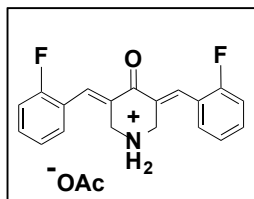

FIG. 2: The 2D structure of the acetate salt of EF24.

The MAC analog, 3,5-bis[(2-fluorophenyl)methylene]-4-piperidinone acetate (EF24, NSC 716993), exhibits broad spectrum activity in both our screening and that of the NCI anticancer 60 cell line panel, as well as potent anti-angiogenic activity in a HUVEC cell migration assay.[23] EF24 has been administered at 10 mg/kg by iv, ip and oral gavage. EF24 plasma stability, protein binding, pharmacokinetics (PK), and metabolism were characterized by LC/MS/MS assays. Plasma protein binding is >98% with preferential binding to albumin. EF24 bioavailability is 60 and 35% after oral and i.p. administration, respectively.[24] After i.p. administration of EF31 at concentrations of 12.5 and 25 mg/kg, peak mouse plasma concentrations were reached at 0.25 and 0.5 hours post-dose (Tmax), respectively. For UBS109 administered at 50 and 150 mg/kg by gavage, peak mouse plasma concentrations were reached at 0.5 and 0.3 hours post-dose (Tmax), respectively. In spite of the fact that UBS109 reduces tumor growth in mice, the compound is quickly metabolized in vitro and 94% protein bound in mouse plasma. The primary monounsatu-

rated metabolite is only modestly bioactive against MDA-MB-231 breast cancer cells. These observations suggest that while the α,β-unsaturated ketone common to curcumin analogs is important for bioactivity, protein binding and tissue distribution may serve to protect UBS109 from full metabolism in vivo, while allowing it to exert a pharmacological effect by means of slow drug release.[8, 25]

We demonstrated that oxidative stress is one of the main mechanisms of anti-cancer activity for MACs. EF24 and UBS109 are electrophilic molecules, α,β-unsaturated ketone Michael acceptors and reversibly bind the sulfhydryl group of cysteine (Michael addition) of target proteins, thereby oxidizing the thiol and inducing oxidative stress, whereas curcumin either does not bind GSH or does so weakly and transiently [26, 27] to act as an overall antioxidant. The redox state of the cell is primarily a consequence of the precise balance between the levels of ROS and endogenous thiol buffers present in the cell, such as glutathione (GSH) and thioredoxin (Trx). EF24-induced oxidative stress is evidenced by an increase of reactive oxygen species (ROS) production, depletion of glutathione GSH, its oxidized form, GSSG, and Trx in cells with and without overexpression of Bcl-XL. Oxidative stress induces mitochondrial membrane depolarization and subsequently activates caspases-9 and -3 activation, surface phosphatidylserine (PS) exposure, DNA fragmentation and apoptotic cell death in both breast and prostate cancer cells.[28, 29] Since Michael addition is one of the key mechanisms of EF24's chemical action, we anticipate that there will be many molecular targets for EF24.[23, 28, 30-32]

While many investigators have documented a variety of bioactions and molecular targets of curcumin [33] and its analogs, the actual target(s) for these drugs are not well defined. Mainly, studies have focused on the ability of curcumin to inhibit the activities of transcription factors such as nuclear factor kappa B (NF-κB).[34-36] Both activator protein 1 (AP-1) and NF-κB have been implicated in the process of carcinogenesis and are constitutively activated in a number of cancer cell lines.[37-39] Several genes that are involved in cellular transformation, proliferation, angiogenesis, invasion, and metastasis are regulated by AP-1 [40] and NF-κB.[38] Thus, modulation of their activity may be an effective strategy against cancer. AP-1 is a heterodimeric transcription factor com-

posed of proteins belonging to the c-Fos, c-Jun, activating transcription factor (ATF) and jun dimerization protein (JDP) families. AP-1 binds to the TRE (TPA DNA responsive element) motif and upregulates transcription of the genes containing TRE. AP-1 regulates gene expression in response to signals generated by a wide array of extracellular stimuli including growth factors, tumor promoters, neurotransmitters, UV light and cytokines and, in addition, controls a number of cellular processes including differentiation, proliferation, and apoptosis.[40] NF-κB is an inducible and ubiquitously expressed transcription factor for genes involved in cell survival, cell adhesion, inflammation, differentiation and growth. Active NF-κB complexes are dimers of various combinations of the Rel family of polypeptides consisting of p50 (NF-κB1), p52 (NF-κB2), c-Rel, v-Rel, Rel A (p65) and Rel B.[38] AP-1 and NF-κB have also been demonstrated to affect the process of apoptosis.[41-47] Apoptosis is characterized by numerous biochemical and morphological changes in the cell including surface PS exposure, caspase activation (particularly caspase-3), cytoplasmic shrinkage and DNA fragmentation. Studies suggest that both oxidative stress and changes in the mitochondrial membrane potential are causal agents of apoptosis.[46, 47]

Mechanistically, MACs (EF24) potently suppress the NF-κB signaling pathway by direct action on IκB kinase (IKK).[48] In a screen of 50 kinases relevant to many forms of cancer, EF31 showed ≥85% inhibition of 10 of the enzymes at 5 μM, while 22 of the proteins were blocked by ≥40%. These MACs are pleiotropic inhibitors that operate at multiple points along cell signaling pathways, show selectivity for serine/threonine kinases and compete with ATP.[49] In a related study, EF24 was found to be a strong inhibitor of FANC-D2-Ub and therefore a regulator of Fanconi anemia (FA). Studies suggest that MAC drugs target the FA pathway through blockade of IKK.[50]

In concert with manipulation of NF-κB in the cytoplasm, EF24-induced decrease of lung cancer cell viability is known to be accompanied by upregulation of mitogen-activated protein kinases (MAPKs) as evidenced by increased phosphorylation of ERK1/2, JNK and p38. Indeed, we have demonstrated that a combination of EF24 and SB203580, a p38 inhibitor, synergistically inhibits clonogenic activity of A549 lung cancer cells while inducing apoptosis and the accumulation of the sub-G$_1$ fraction of cells.[51] In parallel,

EF31 increases basal levels of MAPK transcription factor-DNA binding in mouse RAW264.7 macrophages.[9]

To elucidate a global view of the anticancer/cytocidal actions of these compounds, we sought information regarding their drug targets by using microarrays, and examined cellular localization of EF24 and the activity of two key transcription factors, AP-1 and NF-κB, essential for cell survival and death.

Methods and Materials

Cell culture
Mia-PaCa-2, ASPC-1, Pt45P1, MDA-MB-231, and DU-145 cells were cultured as described.[28, 52, 53] Neutral Red Dye assay was used for the cytotoxic activity of drugs.[8]

Synthesis of biotinylated EF24 analogs
Biotinylated 3,5-bis-(2-fluorobenzylidene)-piperidin-4-one (**Figure 3A**): Under argon, 50.0 mg (0.20 mmol) of D-biotin (**Figure 3C**) and 65.0 mg (0.20 mmol) of the curcumin derivative, 3,5-bis-(2-fluorobenzylidene)-piperidin-4-one, were suspended in 0.6 mL of dimethylyformamide (DMF). Hydroxybenzotriazole (54.0 mg, 0.40 mmol) was added and after cooling the reaction mixture to 0°C, 0.22 mL (1.0 M in CH$_2$Cl$_2$, 0.22 mmol) of 1, 3-dicyclohexylcarbodiimide was added. The reaction mixture was stirred overnight at room temperature. The white solid that formed was filtered off, and the solvent was removed under vacuum. The crude product was purified by preparative HPLC (C18 DYNAMAX column; UV detector 254 nm; 1. run: flow rate: 8 mL, solvent system: 80% water - 20% acetonitrile --> 20% water -80% acetonitrile within 50 minutes, retention time: 38.6 minutes; 2. run: flow rate: 12 mL, solvent system: 70% water – 30% acetonitrile --> 30% water – 70% acetonitrile within 50 minutes, retention time: 37.1 minutes). Yield (crude): 95.7 mg (89%); Yield: 15.1 mg (14%); ^{1}H NMR (400 MHz, CD$_3$COCD$_3$) δ 7.86 - 7.83 (2H, m), 7.64 – 7.50 (4H, m), 7.39 – 7.25 (4H, m), 5.80 (1H, bs), 5.71 (1H, bs), 4.87 (2H, s), 4.82 (2H, s), 4.46 (1H, t, J = 7.6), 4.82 (1H, t, J = 5.2), 3.12 – 3.08 (1H, s), 2.90 (1H, dd, J$_1$ = 12.8, J$_2$ = 5.2), 2.67 (1H, d, J = 12.8), 2.21 (2H, t, J = 7.6), 1.62 – 1.19 (6H, m); ^{13}C NMR (100 MHz, CD$_3$COCD$_3$) δ185.76, 171.45, 163.50, 161.16, 134.78, 132.14, 131.33, 129.07, 124.99, 116.23, 115.87, 61.68, 60.15, 55.764, 46.68, 43.16, 40.33, 32.43, 25.09, 24.95; Fast Atom Bombardment Mass Spectroscopy (FABMS): m/z 544.7 ([M+Li]$^+$, C$_{29}$H$_{29}$F$_2$LiN$_3$O$_3$S requires 544.5).
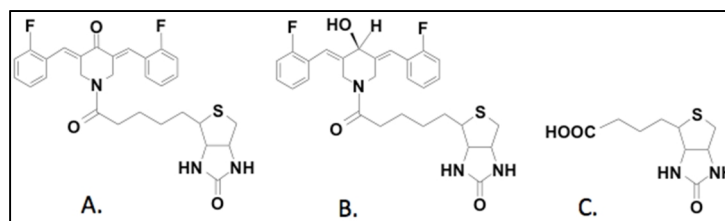

FIG. 3: The structures of biotinylated EF24, C=O reduced biotinylated EF24 analog, and D-biotin.

Biotinylated 3,5-bis-(2-fluorobenzylidene)-piperidin-4-ol (**Figure 3B**) : Under argon, 45.8 mg (186.0 µmol) of cerium (III) chloride was suspended in 1 mL of methanol. At room temperature, 100.0 mg (186.0 µmol) of biotinylated 3,5-bis-(2-fluorobenzylidene)-piperidin-4-one was added to the suspension and followed 5 minutes later by 7.03 mg (186.0 µmol) of sodium borohydride. The reaction mixture was stirred for 30 minutes at room temperature. After filtration, the solvent was removed, and the crude product purified by column chromatography (silica gel, ethyl acetate). A white solid was obtained in 86% yield (86.3 mg). ^{1}H NMR (400 MHz, CD$_3$COCD$_3$) δ 7.53 – 7.50 (2H, m), 7.39 – 7.710 (8H, m), 6.78 (2H, s), 6.05 (1H, bs), 6.01 (1H, bs), 5.89 (1H, s), 4.62 – 4.24 (6H, m), 3.13 – 3.08 (1H, m), 2.91 – 2.87 (1H, m), 2.68 (1H, d, J = 12.8), 2.10 – 2.04 (2H, m), 1.60 – 1.17 (6H, m); ^{13}C NMR (100 MHz, CD$_3$COCD$_3$) δ 171.04, 163.34, 140.92, 131.04, 129.74, 129.30, 124.61, 124. 38, 116.30, 115.87, 115.65, 115.51, 115.29, 74.367, 61.64, 60.16, 55, 79, 45.52, 41.88, 40.33, 32.58, 28.19, 24.94; High Resonance Fast Atom Bombardment Mass Spectroscopy (HRFABMS): m/z 546.221 ([M+Li]$^+$, C$_{29}$H$_{31}$F$_2$LiN$_3$O$_3$S requires 546.221).

Light and confocal microscopy immunohistochemistry

For the light microscopy experiments, MDA-MB-231 breast cancer cells were plated on Lab-Tek 8 chamber glass slides (Nunc, Inc., Naperville, IL). Following an overnight incubation, the cells were treated with DMSO, 10 µM D-Biotin (**Figure 3C**), 10 µM EF24, 10 µM EF24-Biotin (**Figure 3A**) and 10 µM reduced EF24-Biotin (**Figure 3B**) for 6 hours. The media was aspirated and the cells were fixed by adding 2% formaldehyde in PBS for 15 minutes. After a final wash with PBS, the slides were ready to be stained. Avidin-Biotin Complex (ABC) (Vector Laboratories, Burlingame, CA) and 3, 3'-diaminobenzidine tetrahydrochloride (DAB, 0.025%; Sigma Chemical Company, St Louis, MO) staining were carried out according to the procedure of Vector Laboratories. All imaging was performed using a Leica DMRB light microscope (Leica Microsystems, Bannockburn, IL) coupled to a Leica DC500 digital camera system.

For the confocal microscopy experiments, MDA-MB-231 cells were plated on Lab-Tek 8 chamber glass slides. Following an overnight incubation, the cells were treated with 10 µM D-biotin, 10 µM EF24-biotin, and 10 µM reduced EF24-biotin for various periods of time. The media was aspirated and the cells were washed and fixed by adding a solution of 0.5% Triton X-100 and 3.7% formaldehyde in PBS for 15 minutes. After washing twice with PBS, the cells were washed with a solution of 1% BSA in PBS and then prepared for staining. Streptavidin-FITC (Molecular Probes, Eugene, OR) was diluted into the same solution of 1% BSA in PBS and added to the wells for 45 minutes at room temperature. The cells were washed twice with PBS and then once with 2x SSC solution which is diluted from 20x SSC solution. DNAse free, RNAse in 2x SSC solution (final concentration 10 µg/ml) was

then added and the cells were incubated for 20 minutes at 37°C. Next, the cells were washed multiple times with 2x SSC and then the nuclear stain, propidium iodide (Molecular Probes, Eugene, OR), was added to the wells for 5 minutes at room temperature. The cells were washed with 2x SSC solution, and then Antifade equilibration buffer (Molecular Probes, Eugene, OR) was added for 5 minutes. The chambers were then removed, and coverslips were placed on the slides using Antifade reagent. All imaging was performed with the green (488 nm) and red (543 nm) channels of a Zeiss LSM 510 confocal laser scanning microscope (Thornwood, NY) coupled to a Zeiss Axioplan 2 imaging MOT and a 100X plan-Apochromat oil immersion lens.

Measurement of transcription factor binding to DNA

This assay was performed in a manner similar to that previously described.[9, 54-56] DU-145 and MDA-MB-231 cells were grown on 16 cm^2 dishes until 85% confluent. After treatment with EF24 or DMSO for 3 hours, the cells were trypsinized and collected into flow cytometry tubes and centrifuged to obtain a cell pellet. Nuclear extracts were then isolated according to the protocol described by Clontech (Palo Alto, CA) using their Transfactor Nuclear Extraction Kit. The cells were trypsinized and collected into centrifuge tubes, pelleted by spinning for 5 minutes at 1,000 rpm, and the supernatant was discarded. The cells were then rinsed by resuspending in an equal volume of cold PBS, centrifuged (as above), and the supernatant was discarded. Next, the cells were lysed in lysis buffer containing 100 mM HEPES (pH 7.9), 15 mM MgCl$_2$, 100 mM KCl, 0.1M dithiothreitol (DTT), and protease inhibitor cocktail (Sigma, St. Louis, MO) for 15 minutes on ice. After centrifuging the suspension and discarding the supernatant, the cells were disrupted by passing them through a narrow-gauge (No. 27) needle ten times. The disrupted suspension was then centrifuged at 11,000 rpm for 20 minutes, and the supernatant/cytosolic fraction was collected. Next, the crude nuclear pellet was suspended in Extraction Buffer containing 20 mM HEPES (pH 7.9), 1.5 mM MgCl$_2$, 0.42 M NaCl, 0.2mM EDTA, 25% (v/v) glycerol, 0.1 M DTT, and protease inhibitor cocktail and the cells were passed through a narrow gauge (No. 27) needle ten times to disrupt the nuclei. After shaking the nuclear suspension for 30 minutes at 4°C, the suspension was centrifuged at 14,000 rpm for 10 minutes. The supernatant/nuclear fraction was transferred to a clean chilled microfuge tube. The nuclear extracts were then tested for AP-1 and NF-κB transcription factor binding activity according to the procedures of the Transfactor ELISA Kit (BD Clontech, Palo Alto, CA). 30 µg of the nuclear extracts in 1X Transfactor/Blocking Buffer were added to a 96 well plate containing consensus DNA binding sequences for AP-1 and NF-κB. The sequences used were as follows: c-Fos and c-Jun- TGACTCA; NF-κB p50- GGGGATCCC; NF-κB p65- GGGGTATTTCC. Following incubation for 1 hour at room temperature, the wells were washed three times with 1X Transfactor/Blocking Buffer. Primary antibodies for

NF-κB p50, NF-κB p65, c-Fos, and c-Jun were then added to their respective wells and the plate was incubated for 1 hour at room temperature. After washing the wells three times with 1X Transfactor/Blocking Buffer, secondary antibodies were added to the wells. Both Anti-rabbit IgG-HRP and Anti-mouse IgG-HRP were used according to the source of the primary antibody. The wells were then incubated with secondary antibody for 30 minutes at room temperature and washed four times with 1X Transfactor Buffer. Tetra-methylbenzidine (TMB) substrate was then added to the wells for 10 minutes, and the reaction stopped by adding 25 μL of 1M H_2SO_4. The absorbance of the plate was measured at 450 nm with a Bio-Tek microplate reader (Bio-Tek Instruments, Winooski, VT).

Gene microarray

MDA-MB-231 cells were grown on 16 cm^2 dishes to near confluency. The cells were then treated with either DMSO for 24 hours or 2.5 μM EF24 for 4, 14, and 24 hours. Three separate replicates were performed for each of the experimental conditions. Total RNA was then isolated using the RNeasy mini kit from Qiagen (Valencia, CA). The cells were lysed directly in the culture dish using Buffer RLT without β-mercaptoethanol and collected. The samples were then homogenized using QIAshredder spin columns (Qiagen, Valencia, CA), mixed with 70% ethanol, added to RNeasy mini columns, and centrifuged for 15 seconds at 10,000 rpm. The flow-through was discarded, Buffer RW1 added, and the samples were centrifuged as above. This process was then repeated twice using Buffer RPE. To elute the RNA, RNase-free water was added to the RNeasy columns and the samples were centrifuged for 1 minute at 10,000 rpm. The concentration of total RNA was adjusted to a final concentration of 1 μg/μL.

Microarray processing was performed at Expression Analysis, Inc (Durham, NC) using Affymetrix Human U133A Gene Chips according to protocols described in the "Expression Analysis Technical Manual" prepared by Affymetrix, Inc (Santa Clara, CA). The U133A GeneChips contain up to 22,500 probe sets of short oligonucleotides (25mers). Each probe set contains 11-20 pairs of perfect match (PM) oligos and mismatch (MM) oligos that differ by a single nucleotide. Before target production, the quality and quantity of each RNA sample was assessed using an Agilent 2100 BioAnalyzer (Agilent Technologies, Palo Alto, CA). Target was prepared and hybridized. Total RNA (10 μg) was converted into cDNA using reverse transcriptase (Invitrogen, Carlsbad, CA) and a modified oligo (dT) 24 primer that contains T7 promoter sequences (GenSet, San Diego, CA). After first strand synthesis, residual RNA was degraded by the addition of RNAse H and a double stranded cDNA molecule was generated using DNA polymerase I and DNA ligase. The cDNA was purified and concentrated using a phenol:choloform extraction followed by ethanol precipitation. The cDNA products were incubated with T7 RNA polymerase and biotinylated ribo-

nucleotides using an In Vitro Transcription kit (Enzo Diagnostics, Farmingdale, NY). One-half of the cRNA product was purified using an RNeasy column (Qiagen, Valencia, CA) and quantified with a spectrophotometer. The cRNA target (20 μg) was incubated at 94°C for 35 minutes in fragmentation buffer (Tris, MgOAc, KOAc). The size of the fragmented target was confirmed using an Agilent 2100 BioAnalyzer (Agilent Technologies, Palo Alto, CA). The fragmented cRNA was diluted in hybridization buffer (MES, NaCl, EDTA, Tween 20, Herring Sperm DNA, Acetylated BSA) containing biotin-labeled OligoB2 and Eukaryotic Hybridization Controls (Affymetrix, Santa Clara, CA). The hybridization cocktail was denatured at 99°C for 5 minutes, incubated at 45°C for 5 minutes and then injected into a prehybridized GeneChip cartridge. The GeneChip array was incubated at 42°C for at least 16 hours in a rotating oven at 60 rpm. GeneChips were washed with a series of nonstringent and stringent solutions containing variable amounts of MES, Tween 20, and SSPE. The microarrays were then stained with streptavidin phycoerythrin, and the fluorescent signal was amplified using a biotinylated antibody solution. Fluorescent images were detected in an Agilent Gene Array Scanner (Agilent Technologies, Palo Alto, CA).

Statistical considerations

The expression data was extracted using the MicroArray Suite software, version 5.0 (Affymetrix, Santa Clara, CA) and analyzed with a custom Two-Group Comparison program developed at Expression Analysis. The comparison software removes transcripts that were declared "Absent" in all samples and calculates fold change and statistical significance between groups of samples using the Student's t-test.

Results

In vitro potency of EF24 and UBS109: comparison to gemcitabine and Akt/MAPK p38 inhibitors

Our groups have a long-standing interest in pancreatic ductal adenocarcinoma (PDA), a highly lethal form of cancer for which gemcitabine is currently used as a standard chemotherapeutic regimen. PDA pathobiology is marked by high exposure of surface PS and up-regulation of full-length Tissue Factor (flTF), an obligatory enzymatic cofactor for serine protease fVIIa and the main trigger of blood clotting which, together with high surface PS levels, is believed to be major contributing factors to high rates of thrombosis in PDA.[57] We recently showed that a minimally coagulant alternatively spliced form of TF (asTF), also expressed at high levels in PDA lesions, promotes tumor growth and spread non-proteolytically, acting as an integrin ligand.[52] Because both flTF and asTF contribute to tumor growth and spread, as does PS, we sought to examine whether EF24 and/or UBS109 exhibit cytotoxic activity against four human PDA lines: Mia-PaCa-2 (high surface PS, no fl/asTF); ASPC-1(low surface PS, more flTF than asTF); Pt45P1 (medium surface PS,

more flTF than asTF), and Pt45P1/asTF+ (medium surface PS, flTF approximately equals asTF).[52, 53, 58, 59] As shown in **Figure 4**, EF24 as well as UBS109 exerts a significantly more potent effect on all four PDA lines compared to gemcitabine, Akt inhibitor MK-2206, and p38 MAPK inhibitor SB203580.
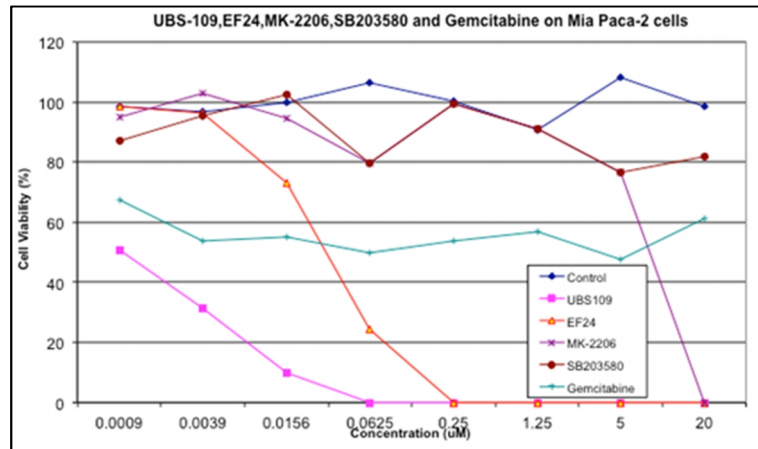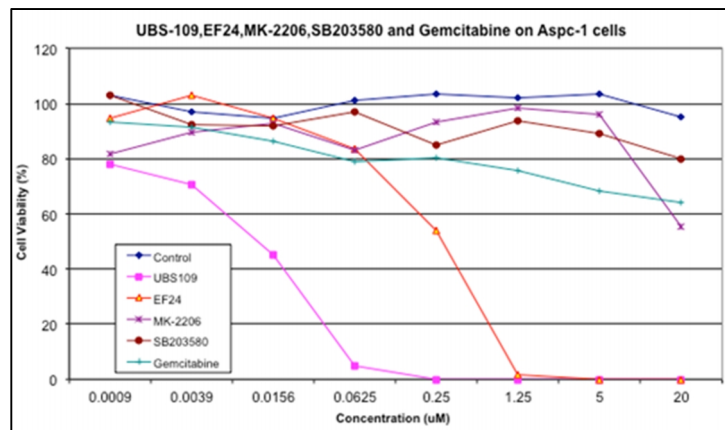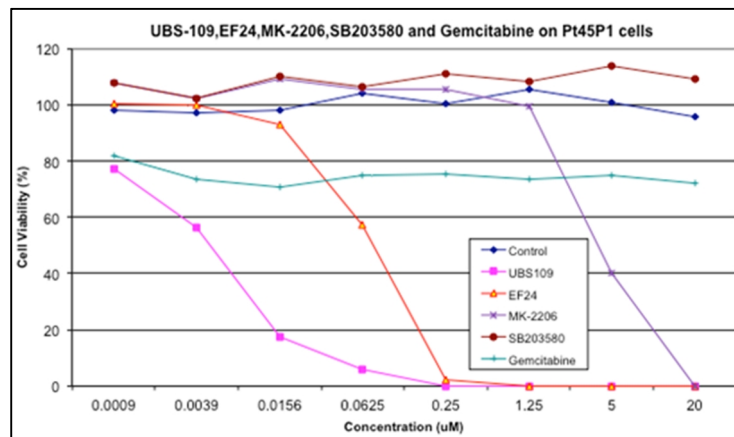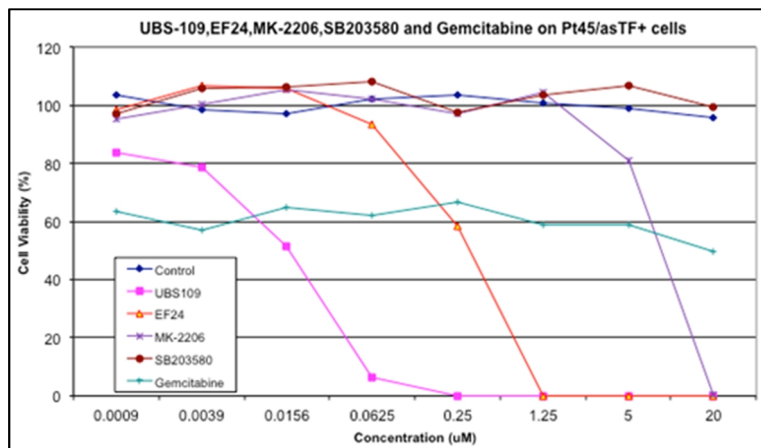

FIG. 4(a)

FIG. 4(b)

FIG. 4(c)

FIG. 4(d)

FIG. 4: UBS109 and EF24 show more potent anti-cancer activity against PDA cells than gemcitabine. Effects of EF24, UBS109, gemcitabine and inhibitors of Akt (MK-2206) and p38 MAPK (SB203580) against various PDA cell lines. (**a**) MiaPaCa-2, high surface PS, no fl/asTF; (**b**) ASPC-1, low surface PS, more flTF than asTF; (**c**) Pt45p1, medium surface PS, more flTF than asTF; and (**d**) Pt45P1/asTF+, medium surface PS, flTF approximately equals asTF.

Using a cell viability assay using Neutral Red Dye in vitro, we compared UBS109 (pink) and EF24 (red) against other chemotherapeutic agents, namely, gemcitabine (blue) used as a *standard chemotherapeutic regimen* for treatment of pancreatic cancer, inhibitors of Akt (MK-2206, purple) and p38 MAPK (SB203580, brown) and vehicle control (navy blue). All agents were dosed from 0.0009 to 20 μM.

EF24, EF31 and UBS109 do not kill normal MCF-10A breast cells at the concentrations ranged from 0.0012 to 20 μM (100% viable). EF24, EF31 and UBS109 are cytotoxic against all cancer cells we tested. UBS109 is the most active and killed 100% at the concentrations indicated in parenthesis after cancer type, including KB-3-1 (squamous cell carcinoma; SCC) (UBS109, 1.2 μM), TU212 (SCC) (5 μM), MiaPaCa-2 (pancreatic cancer) (0.312 μM), SE-MEL-28 (melanoma) (0.070 μM), RPMI-7951 (melanoma) (0.0195 μM), MDA-MB-231 (breast) (0.312 μM), i.e., at concentrations ranging from 0.0012 uM to 20 uM.[8]

Cellular localization of biotinylated EF24

After treatment with a biotinylated drug, a number of techniques employing avidin and streptavidin can be used to identify the cellular localization of the drug as well as its molecular target(s). In order to identify the cellular localization of EF24, biotin was attached to the compound (**Figure 3A**) and light and confocal microscopy were used to visualize the cellular localization of the biotinylated molecule. It is important to mention that the activity of the biotinylated version of EF24 is comparable to that of the parent EF24 (data not shown). MDA-MB-231 and DU-145 cells also express flTF and/or asTF, possess PS-dependent TF activity, and are used extensively in breast and prostate cancer research, respectively.[60-62] In light of breast and prostate cancer prevalence in the general population, we elected to conduct our further studies using MDA-MB-231 and DU-145 cells. **Figure 5** shows MDA-MB-231 cells treated with 10 μM EF24-biotin for 6 hours and visualized using light microscopy. Intense brown DAB staining seen in the nuclei of the cells indicates that the compound enters the cell and binds to a target in the nucleus (**Figure 5D**). The binding of EF24-biotin requires the presence of EF24 since the biotin molecule (**Figure 3C**) itself shows very little staining (**Figure 5B**). In addition, the binding of EF24-biotin is specific, since the staining can be blocked by an excess of EF24 (**Figure 5E**).
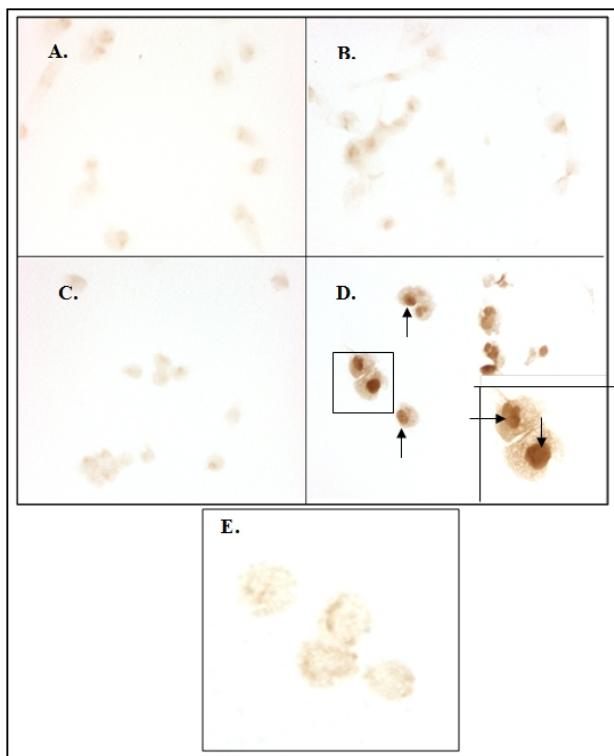

FIG.5: Determination of the cellular localization of biotinylated EF24 using light microscopy.

MDA-MB-231 cells were treated with DMSO (A) 10 μM biotin; (B) 10 μM EF24; (C) 10 μM biotinylated-EF24 for 6 hours (D). The cellular localization of the agents was visualized using DAB (brown stain) at 40X (times) magnification and 60X (times) magnification (inset in D). Brown staining can be seen in the nuclei of the cells in D (see arrows) indicating the likelihood of a nuclear target. Only slight background staining can be seen in A-C, demonstrating that EF24 is necessary for binding. In order to test the specificity of the biotinylated drug, the cells were pretreated with 200 μM EF24 for 30 minutes prior to treatment with 10 μM EF24-biotin for 6 hours (E).
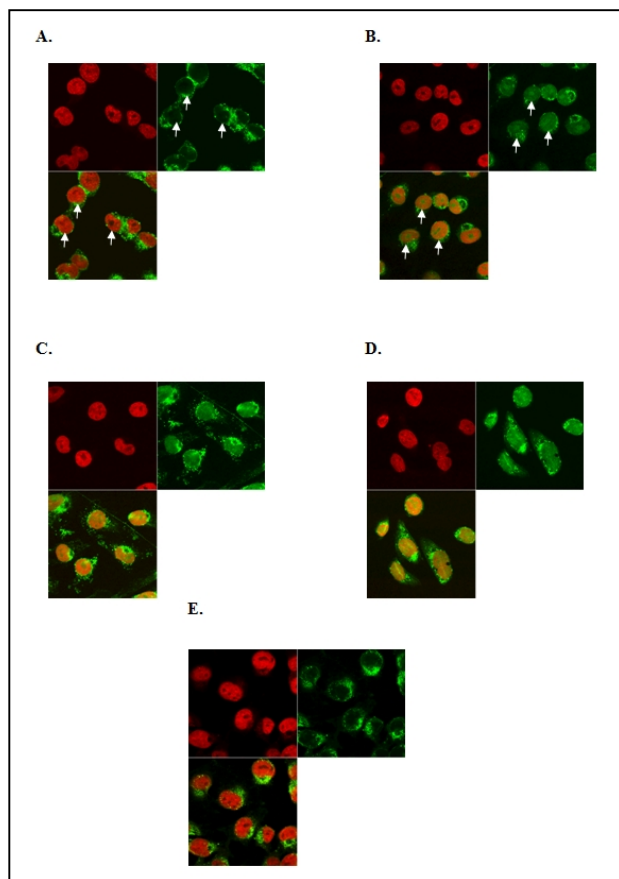

FIG. 6: Determination of the cellular localization of biotinylated EF24 using confocal microscopy.

The localization of the drug in the nucleus was further confirmed by experiments using confocal microscopy. **Figure 6** shows MDA-MB-231 cells treated with 10 μM EF24-biotin at various times and visualized using streptavidin-FITC. Green staining in the nuclei of the cells could be seen after only 30 minutes, and the intensity of the stain increased after 3 and 6 hours treatments (**Figure 6B, 6C, 6D**). This stain overlapped with propidium iodide (PI), which is a well-known nuclear stain. This suggests that the molecular target of EF24 is most likely a nuclear protein(s) and/or DNA; however, see below. The cells were treated with 10 μM D-biotin as a control, and no green color could be seen in the nuclei of the cells (**Figure**

6A). In addition, a reduced derivative of EF24 that can no longer act as a Michael acceptor was also biotinylated (**Figure 3B**). Since a key chemical action of EF24 is the covalent and often reversible attachment of drug to protein through Michael addition, the reduced EF24 derivative was used to probe whether this activity is necessary for cellular localization of the drug. Treatment of cells with the latter produced a staining pattern similar to control, suggesting that this compound does not bind to cellular molecules (**Figure 6E**).

MDA-MB-231 cells were treated with biotin alone (A) 10 μM biotinylated-EF24 for 30 minutes; (B) 3 hours; (C) 6 hours; (D) or 10 μM reduced EF24-biotin for 6 hours (E). The cellular localization of the drugs was visualized using streptavidin-FITC (green fluorescence) and the nuclei of the cells were stained using propidium iodide (PI) (red fluorescence) at 100X magnification. Each panel shows PI alone (top left), streptavidin-FITC alone (top right), and both stains together (bottom left). Panel B shows green staining in the nuclei of the cells treated with EF24-biotin for 30 minutes that is not present in the biotin-treated cells (Panel A) and the overlap of the green and red stains produces an orange color in the nuclei instead of red (see arrows). After 3 hours and 6 hours treatment with EF24-biotin (Panels C and D), the green staining in the nuclei has increased and, consequently, the overlap of the green and red stains produces a bright orange color. Panel E shows that reducing the ketone moiety in EF24 to an alcohol produces a staining pattern that is similar to that of control (Panel A), suggesting that the conjugated carbonyl is important for drug action.

Inhibition of NF-κB activity

NF-κB has been shown to be constitutively activated in many cancer cell lines, including DU-145 and MDA-MB-231.[42, 43] Several laboratories have demonstrated that curcumin is an inhibitor of NF-κB DNA binding activity.[34-36, 43] It has also been established that curcumin does not directly inhibit NF-κB-inducing kinase (NIK) or IκB kinase (IKK) activity, but instead inhibits an upstream signal of NIK leading to IKK activity.[63] Activated NIK then phosphorylates and activates the IKK complex. IKK is part of a multiprotein complex that contains IKK-α and IKK-β subunits, both critical in mediating in vitro cytokine-induced IκB phosphorylation.

We studied the effects of curcumin and EF24 on the DNA binding activity of NF-κB using an ELISA format. This assay is an effective measurement of transcription factor binding in nuclear extracts of treated cells, producing similar results to electrophoretic mobility shift assays (EMSA).[54-56] The outcomes in **Figure 7** indicate that treatment of MDA-MB-231 cells and DU-145 cells with EF24 (10 μM) for 3 hours significantly inhibits the constitutive binding activity of both the p50 and p65 subunits of NF-κB. Curcumin also inhibits NF-κB DNA binding.

MDA-MB-231 cells (A and B) and DU-145 cells (C and D) were treated with 40 µM curcumin or 10 µM EF24 for 3 hours and nuclear extracts were isolated and tested for NF-κB (p65 and p50 subunits) DNA binding activity as described in Materials and Methods. 500 ng of competitor oligonucleotide was added to demonstrate the specificity of the binding reaction. Bars indicate mean ± SEM (n = 2- 4) of transcription factor binding activity (absorbance 450 nm). Significant difference from control is denoted as * $P < 0.05$, ** $P < 0.01$, *** $P < 0.001$.

Induction of c-Fos/AP-1 activity

Since the antiproliferative effects of curcumin have been attributed to an anti-AP-1 activity [34-36], we studied the effects of our MAC on the DNA binding activity of this transcription factor using the Transfactor ELISA assay as was used for NF-κB. The treatment of breast and prostate cancer cells with EF24 for 3 hours produced a more than 5-fold increase in the DNA binding activity of c-Fos instead of a decrease in the activity of AP-1 (**Figure 8**). However, the addition of EF24 to a previously untreated nuclear extract did not increase c-Fos or c-Jun binding activity in the ELISA assay, indicating that the compound most likely effects the upstream activation of the transcription factor and does not directly interfere with DNA binding. In the same assay, curcumin, on the other hand, inhibited both c-Jun and c-Fos in both cell lines, confirming results seen by others using the EMSA method.[34, 35, 64]

MDA-MB-231 cells (A and B) and DU-145 cells (C and D) were treated with 40 µM curcumin or 10 µM EF24 for 3 hours and nuclear extracts were isolated and tested for c-Fos and c-Jun DNA binding activity as described in Methods and Materials. 500 ng of competitor oligonucleotide was added to demonstrate the specificity of the binding reaction. Bars indicate mean ± SEM (n = 2 - 4) of transcription factor binding activity (absorbance 450 nm). Significant difference from control is denoted as * $P < 0.05$, ** $P < 0.01$, *** $P < 0.001$.

Effect of EF24 on cancer-related gene expression

Table 1 shows a list of cancer-related genes affected by EF24. Genes important for angiogenesis, migration and metastasis, such as interleukin-1 beta (IL-1β), interleukin-6 (IL-6), interleukin-8 (IL-8), VEGF, urokinase plasminogen activator (uPA) and cyclooxygenase-2 (COX-2), were all down regulated after 4 hours EF24 treatment. Because all these genes have been shown to be regulated by NF-κB [42], this decrease in transcript levels supports the results in **Figure 7** demonstrating that EF24 indirectly decreases the DNA binding activity of NF-κB. Modulation of these genes may play a role in the ability of EF24 to induce apoptosis and reduce breast tumor size in vivo.[28]
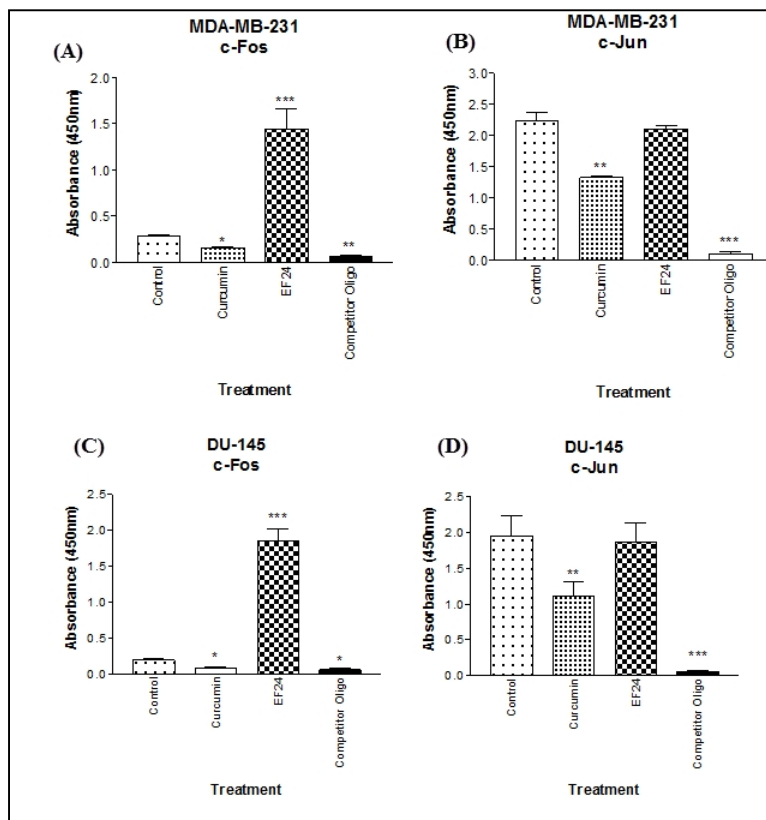

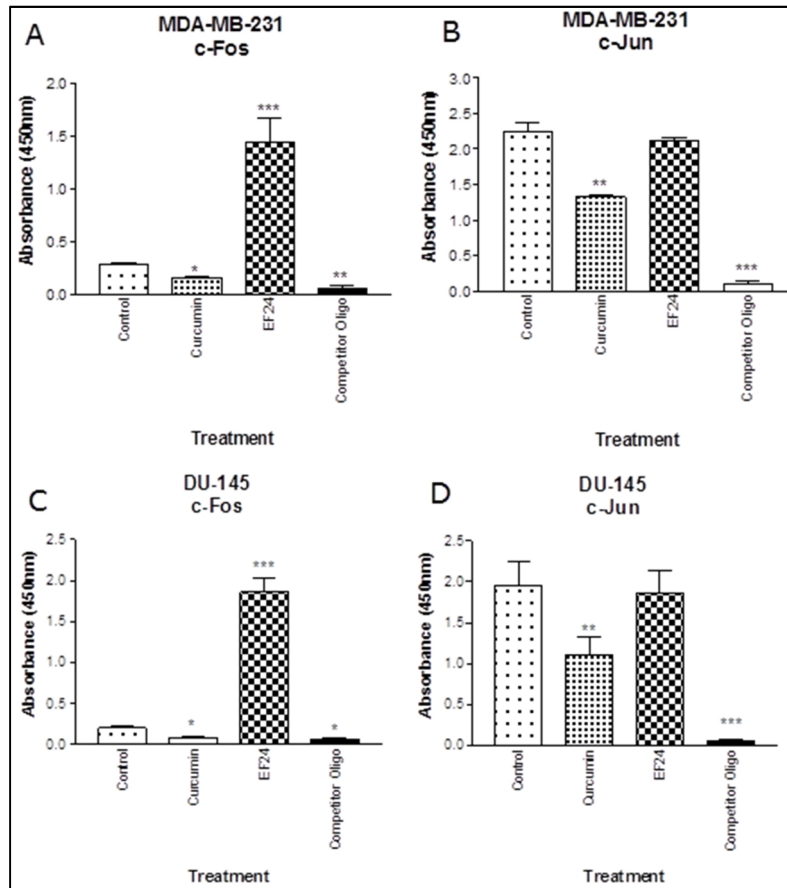**FIG. 7:** EF24 inhibits the DNA binding activity of NF-κB.

FIG. 8: EF24 activates the DNA binding activity of c-Fos/AP-1.

TABLE 1: Modulation of cancer-related genes by EF24.

Genes	Fold Change	Time	Function
Interleukin-1, beta	-1.75	4h	Angiogenesis, Osteoclast Activation
Interleukin-6	-2.12	4h	Migration, Angiogenesis, Metastasis
Interleukin-8	-2.85	4h	Angiogenesis
Vascular Endothelial Growth Factor	-1.64	4h	Angiogenesis
Urokinase Plasminogen Activator	-1.95	4h	Invasion, Migration, Metastasis
Cyclooxygenase-2	-2.55	4h	Proliferation, Angiogenesis, Metastasis
Heme Oxygenase-1	+22.6	4h	Cytoprotection/Anti-carcinogenesis
Quinone Reductase	+1.86	4h	Cytoprotection/Anti-carcinogenesis
Quinone Reductase	+2.13	14h	
Quinone Reductase	+2.01	24h	

Treatment of the cells with EF24 also induced the upregulation of genes that play a role in cytoprotection and anti-carcinogenic activity. Strikingly, a 22-fold increase was seen in the heme oxygenase-1 (HO-1) transcript after 4 hours. HO-1 is an enzyme that contributes to the conversion of heme to bilirubin, a bile pigment and active antioxidant. In addition, treatment of the cells with EF24 induced a 2-fold increase in the NAD (P) H quinone reductase gene (QR) after 4 hours, and this upregulation persisted over 14 hours (+2.13) and 24 hours (+2.01). Quinone reductase is a phase II detox-ifying enzyme that is important in fighting chemical carcinogens. Both of these genes are regulated by AP-1 [64, 65]; thus, this increase in transcript level supports the results in **Figure 8**, which show that EF24 induces AP-1 activity. The microarray data show that EF24 also increases gene expression of several stress genes such as heat shock proteins (HSP)-40 (+2.4), HSP-60 chaperonin (+2.3), HSP-70 (+3.0), HSP-90 (+1.86), thioredoxin interacting protein (+2.28), and glucocorticoid receptor DNA binding protein (+2.5). Acting in

concert, these genes may help the cells to survive oxidative stress.

Discussion

We show here that EF24 and UBS109 are significantly more cytotoxic against four PDA cancer cell lines compared to gemcitabine. Our immunohistochemical studies reveal that biotinylated EF24 rapidly localizes to the nuclei, while its reduced biotinylated variant does not. This suggests that the conjugated compound affects DNA binding activity of NF-κB and c-Fos in the nuclear compartment of MDA-MB-231 and DU-145 cells.

EF24 reduces the levels of DNA binding of both NF-κB p65 and p50 subunits and increases that of c-Fos, as demonstrated by ELISA of the nuclear extracts from EF24-treated cells.[9, 54-56] These results are consistent with the data previously demonstrating that EF24 blocks NF-κB by suppressing IKK [37], while curcumin inhibits NF-κB by blocking the pathway upstream of NIK and IKK.[63] However, EF24 has no effect on the DNA binding activity of c-Fos when added directly to the untreated-nuclear extracts from either of the cell lines. EF24 increases the DNA binding of c-Fos, while curcumin (curcumin-loaded polyvinylpyrrolidone nanoparticles), by contrast, inhibits both c-Fos and c-Jun, hence AP-1 binding.[66]

The precise molecular details are not yet in hand, but we propose a hypothesis as to the basis for the staining of nuclear proteins by biotinylated EF24, and the possibility that EF24 and related anti-cancer agents can relieve tumorigenic effects by action in the nucleus. It appears that Michael addition is necessary for EF24 to interact with its molecular target(s), suggesting that its cytocidal actions and anti-proliferative effects are dependent upon this mechanism. As to potential targets of EF24, cysteine dioxygenase type 1, (CDO1), is a DNA hypermethylated gene that determines the flux between cysteine catabolism and glutathione synthesis. Inactivation of CDO1 contributes to cancer cell survival.[67] EF24 may not only capture glutathione and thioredoxin by Michael addition [23, 28, 29] but the two closely related analogs (EF31 and UBS109) are known to serve as DNA hypomethylating agents in pancreatic cancer.[10] Such drug action suggests the capacity for silencing of CDO1 by reduction or reversal of methylation. Furthermore, it is well-known that plant homeodomain (PHD) zinc fingers, characterized by the Cys4-His-Cys3 motif, are able to serve as epigenome readers controlling gene expression via recruitment of multiprotein complexes of chromatin regulators and transcription factors.[68] EF24 and its congeners have the ability to disrupt zinc fingers by Michael-guided alkylation of the cysteines in the Cys4-His-Cys3 triads. Thus, several chemical actions dependent on Michael addition may account for our observations.

EF24 is an oxidant: it operates as a Michael acceptor and binds GSH and thioredoxin via cysteine sulfhydryl groups and induces oxidative stress leading to an increase in binding of DNA and c-Fos/AP-1. Curcumin behaves as a phenolic anti-oxidant inducing anti-inflammatory action, and as a pro-oxidant that causes apoptosis. As an anti-oxidant, it quenches ROS and thus reduces free radical reacting capacities. Conversely, the pro-oxidant activity of curcumin is dependent on the generation of ROS that induces apoptosis. The mechanisms underlying these two opposite activities are complex, and the two structures of curcumin (keto and enolic forms) in solution, position of the hydroxyl group in the aromatic ring, the presence of transition metal ions, route of administration, and localized tissue are vital decisive factors in determining curcumin's behavior.[69]

We postulate that the primary anti-cancer action of EF24 is to cause cellular oxidative stress and induce apoptosis at low µM concentrations. Further increases in concentration may lead to rapid cell death predominantly via necrosis, similar to that induced by phenethyl isothiocyanate (PEITC), found in cruciferous vegetables, and butylated hydroxyanisole (BHA), a dietary chemopreventive compound.[70-71]

A second important anti-cancer action of EF24 is inhibition of NF-κB. We previously demonstrated that EF24 inhibits this transcription-regulating protein complex by inhibiting IKK in the cytoplasm.[37] The activities of MACs on various kinases were screened using a 50-kinase panel of the Z' Lyte in vitro kinase assay. Among MACs, EF31 more actively inhibits multiple serine/threonine kinases, most prominently IKKβ, Akt and kinase insert domain receptor (KDR, a type III receptor tyrosine kinase) also known as vascular endothelial growth factor receptor 2 (VEGFR-2). However, EF31 was not active against p38 and ERK2.[38] Gene microarray analysis of EF24 demonstrated that the compound significantly inhibits downstream genes of NF-κB transcriptional activation such as IL1-β, IL-6, IL-8, VEGF and COX-2.

Why should the anticancer drug EF24 increase the DNA-binding of c-Fos, consequently activate AP-1 and promote cancer growth and, thereby, counteract the anticancer action of the drug itself? One explanation is that cells may respond to chemical insult to counteract oxidative stress in an attempt to simultaneously protect the cells. Support for this hypothesis can be found in the examples cited below.

PEITC, one of many compounds found in cruciferous vegetables, induces a dose-dependent decrease in cell viability through induction of cell apoptosis and cell cycle arrest in the G(2)/M phase of DU-145 cells, as does EF24. Both molecules are electrophiles (as is a Michael acceptor) and interact with thiols such as GSH. PEITC causes mitochondrial dysfunction, increases the release of cytochrome c and endonuclease G (an apoptotic DNAse) from mitochondria, and guides cell apoptosis via mitochondria-dependent signaling pathway.[70] Dietary chemopreventive compounds (isothiocyanates and green tea polyphenols), phenolic antioxidants such as BHA and its

metabolite, t-butyl-hydroquinone (tBHQ) used in food preservatives, naturally occurring phytochemicals, such as PEITC and sulfarophane typically generate cellular oxidative stress. They modulate gene expression including phase II detoxifying enzymes glutathione-s-transferase (GST) and NAD (P) H-quinone reductase (QR) and HO-1 via the antioxidant/electrophile response element (ARE/EpRE).[71] We note that ARE is composed of two adjacent AP-1-like binding sites and can be activated by Fos/Jun.[64]

The induction of HO-1 by EF24 parallels a decrease in intracellular GSH, while a sustained reduction in GSH increases HO-1. In support of this hypothesis, it has been demonstrated that treatment with the antioxidants N-acetyl-L-cysteine (NAC) or GSH reduces the expression of HO-1 induced by cigarette smoke extract (CSE) exposure. AP-1 is a redox-sensitive transcription factor shown in other systems to regulate HO-1 expression. CSE exposure results in nuclear accumulation of c-Fos and c-Jun, two key AP-1 components. Reduction of c-Fos and c-Jun nuclear translocation by the JNK inhibitor SP-600125 attenuated the CSE-induced expression of HO-1.[72]

Finally, the MAC class of compounds differentially activates the mitogen-activated protein kinases (MAPK; ERK, JNK and p38) involved in the transcriptional activation of the ARE-mediated reporter gene. N-acetyl-L-cysteine, GSH and vitamin E inhibit ERK2 activation and, to a much lesser extent, JNK 1 activation by BHA and tBHQ, pointing to the role of oxidative stress. It was suggested that low concentrations of these chemicals (e.g., BHA, PEITC) activate MAPKs leading to induction of gene expression (e.g., c-jun, c-fos), which may protect the cells against toxic insults / enhance cell survival. At relatively high concentrations, these agents activate both MAPKS and the ICE/Ced-3 caspase pathway, leading to apoptosis. Further increase in concentrations leads to rapid cell death occurring mainly via necrosis [73]; cancer cells seem to respond to EF24 by increasing the DNA binding of c-Fos and gene expression of several stress genes in a manner similar to these agents.

Conclusion

In conclusion, we have demonstrated that EF24 increases the DNA binding of c-Fos. Our data suggest that EF24 triggers a negative feedback loop through p38 activation to protect cell survival, which is in agreement with the observation that a combination of EF24 and SB203580, a p38 inhibitor, synergistically blocks clonogenic activity of cancer cells and induces their apoptosis.[40] Modulation of these transcription factors may reflect cell responses indicative of a struggle for survival in the process of cell death due to oxidative stress by EF24. However, the protective actions in cancer cells are unable to prevail against the insult of oxidative stress, which induces depolarization of the mitochondrial membrane leading to apoptosis.

Conflict of interest

The authors declare that they have no conflicts of interest. The authors alone are responsible for the content and writing of the paper.

Acknowledgment

References

1. Aggarwal BB, Kumar A, Bharti AC. Anticancer potential of curcumin: preclinical and clinical studies. *Anticancer Res* 2003; **23**:363-98.

2. Satoskar RR, Shah SJ, Shenoy SG. Evaluation of anti-inflammatory property of curcumin (diferuloyl methane) in patients with postoperative inflammation. *Int J Clin Pharmacol Ther Toxicol* 1986; **24**:651-4.

3. Wang YJ, Pan MH, Cheng AL, *et al.* Stability of curcumin in buffer solutions and characterization of its degradation products. *J Pharm Biomed Anal* 1997; **15**:1867-76.

4. Shen L, Ji HF. The pharmacology of curcumin: is it the degradation products? *Trends Mol Med* 2012; **18**:138-44.

5. Shetty D, Kim YJ, Shim H, Snyder JP. Eliminating the heart from the curcumin molecule: monocarbonyl curcumin mimics (MACs). *Molecules* 2014; **20**:249-92.

6. Zhou T, Ye L, Bai Y, *et al.* Autophagy and apoptosis in hepatocellular carcinoma induced by EF25-(GSH)2: a novel curcumin analog. *PLoS One* 2014;**9**:e107876.

7. Zhu S, Moore TW, Lin X, *et al.* Synthetic curcumin analog EF31 inhibits the growth of head and neck squamous cell carcinoma xenografts. *Integr Biol (Camb)* 2012;**4**:633-40.

8. Zhu S, Moore TW, Morii N, *et al.* Synthetic curcumin analog UBS109 inhibits the growth of head and neck squamous cell carcinoma xenografts. *Curr Cancer Drug Targets* 2014;**14**:380-93.

9. Olivera A, Moore TW, Hu F, *et al.* Inhibition of the NF-κB signaling pathway by the curcumin analog, 3,5-Bis(2-pyridinylmethylidene)-4-piperidone

(EF31): anti-inflammatory and anti-cancer properties. *Int Immunopharmacol* 2012;**12**:368-77.

10. Nagaraju GP, Zhu S, Wen J, *et al*. Novel synthetic curcumin analogues EF31 and UBS109 are potent DNA hypomethylating agents in pancreatic cancer. *Cancer Lett* 2013;**341**:195-203.

11. Yamaguchi M, Moore TW, Sun A, *et al*. Novel curcumin analogue UBS109 potently stimulates osteoblastogenesis and suppresses osteoclastogenesis: involvement in Smad activation and NF-κB inhibition. *Integr Biol (Camb)* 2012; **4**:905-13.

12. Yamaguchi M, Zhu S, Weitzmann MN, *et al*. Curcumin analog UBS109 prevents bone marrow osteoblastogenesis and osteoclastogenesis disordered by coculture with breast cancer MDA-MB-231 bone metastatic cells in vitro. *Mol Cell Biochem* 2015;**401**:1-10.

13. Selvendiran K, Tong L, Vishwanath S, *et al*. EF24 induces G2/M arrest and apoptosis in cisplatin-resistant human ovarian cancer cells by increasing PTEN expression. *J Biol Chem* 2007; **282**:28609-18.

14. Subramaniam D, May R, Sureban SM, *et al*. Diphenyl difluoroketone: a curcumin derivative with potent in vivo anticancer activity. *Cancer Res* 2008; **68**:1962-9.

15. Liang Y, Zheng T, Song R, *et al*. Hypoxia-mediated sorafenib resistance can be overcome by EF24 through Von Hippel-Lindau tumor suppressor-dependent HIF-1α inhibition in hepatocellular carcinoma. *Hepatology* 2013; **57**:1847-57.

16. Nagaraju GP, Zhu S, Ko JE, *et al*. Antiangiogenic effects of a novel synthetic curcumin analogue in pancreatic cancer. *Cancer Lett* 2015; **357**:557-65.

17. Thomas SL, Zhong D, Zhou W, *et al*. EF24, a novel curcumin analog, disrupts the microtubule cytoskeleton and inhibits HIF-1. *Cell Cycle* 2008; **7**:2409-17.

18. Sun A, Shoji M, Lu YJ, *et al*. Synthesis of EF24-tripeptide chloromethyl ketone: a novel curcumin-related anticancer drug delivery system. *J Med Chem* 2006; **49**:3153-8.

19. Shoji M, Sun A, Kisiel W, *et al*. Targeting Tissue Factor-Expressing Tumor Angiogenesis and Tumors with EF24 Conjugated to Factor VIIa. *J Drug Target* 2008; **16**:185-97.

20. Ndungu JM, Lu YJ, Zhu S, *et al*. Targeted delivery of paclitaxel to tumor cells: synthesis and in vitro evaluation. *J Med Chem* 2010; **53**:3127-32.

21. Zhu S, Kisiel W, Lu YJ, *et al*. Visualizing cancer and response to therapy in vivo using Cy5.5-labeled factor VIIa and anti-tissue factor antibody. *J Drug Target* 2015;**23**:257-65.

22. Zhu S, Kisiel W, Lu YJ, *et al*. Tumor angiogenesis therapy using targeted delivery of Paclitaxel to the vasculature of breast cancer metastases. *J Drug Deliv* 2014;**2014**:865732.

23. Adams BK, Ferstl EM, Davis MC, *et al*. Synthesis and biological evaluation of novel curcumin analogs as anti-cancer and anti-angiogenesis agents. *Bioorg Med Chem* 2004;**12**:3871-83.

24. Reid JM, Buhrow SA, Gilbert JA, *et al*. Mouse pharmacokinetics and metabolism of the curcumin analog, 4-piperidinone,3,5-bis[(2-fluorophenyl) methylene]-acetate(3E,5E) (EF-24; NSC 716993). *Cancer Chemother Pharmacol* 2014;**73**:1137-46.

25. Moore TW, Zhu S, Randolph R, *et al*. Liver S9 Fraction-Derived Metabolites of Curcumin Analogue UBS109. *ACS Med Chem Lett* 2014;**5**: 288-92.

26. Usta M, Wortelboer HM, Vervoort J, *et al*. Human Glutathione S-Transferase-Mediated Glutathione Conjugation of Curcumin and Efflux of These Conjugates in Caco-2 Cells. *Chem Res Toxicol* 2007; **20**:1895-902.

27. Awasthi S, Pandya U, Singhal SS, *et al*. Curcumin-glutathione interactions and the role of human glutathione S-transferase P1-1. *Chem Biol Interact* 2000;**128**:19-38.

28. Adams BK, Cai J, Armstrong J, *et al*. EF24, a novel synthetic curcumin analog, induces apoptosis in cancer cells via a redox-dependent mechanism. *Anticancer Drugs* 2005;**16**:263-75.

29. Sun A, Lu YJ, Hu H, *et al*. Curcumin analog cytotoxicity against breast cancer cells: exploitation of a redox-dependent mechanism. *Bioorg Med Chem Lett* 2009;**19**:6627-31.

30. Johansson MH. Reversible Michael additions: covalent inhibitors and prodrugs. *Mini Rev Med Chem* 2012;**12**:1330-44.

31. Serafimova IM, Pufall MA, Krishnan S, et al. Reversible targeting of noncatalytic cysteines with chemically tuned electrophiles. *Nat Chem Biol* 2012;**8**:471-6.

32. Potashman MH, Duggan ME. Covalent modifiers: an orthogonal approach to drug design. *J Med Chem* 2009;**52**:1231-46.

33. Gupta SC, Prasad S, Kim JH, et al. Multitargeting by curcumin as revealed by molecular interaction studies. *Nat Prod Rep* 2011;**28**:1937-55.

34. Pendurthi UR, Williams JT, Rao LV. Inhibition of tissue factor gene activation in cultured endothelial cells by curcumin. Suppression of activation of transcription factors Egr-1, AP-1, and NF-kappa B. *Arterioscler Thromb Vasc Biol* 1997;**17**:3406-13.

35. Bierhaus A, Zhang Y, Quehenberger P, *et al*. The dietary pigment curcumin reduces endothelial tissue factor gene expression by inhibiting binding of AP-1 to the DNA and activation of NF-kappa B. *Thromb Haemost* 1997;**77**:772-82.

36. Singh S, Aggarwal BB. Activation of transcription factor NF-kappa B is suppressed by curcumin (diferuloylmethane) [corrected]. *J Biol Chem* 1995; 270:24995-5000. Erratum in: 1995;270:30235.

37. Chen TK, Smith LM, Gebhardt DK, *et al*. Activation and inhibition of the AP-1 complex in human breast cancer cells. *Mol Carcinog* 1996;15:215-26.

38. Nakshatri H, Goulet RJ Jr. NF-kappaB and breast cancer. *Curr Probl Cancer* 2002;26:282-309.

39. Mukhopadhyay A, Bueso-Ramos C, Chatterjee D, *et al*. Curcumin downregulates cell survival mechanisms in human prostate cancer cell lines. *Oncogene* 2001;20:7597-609.

40. Angel P, Karin M. The role of Jun, Fos and the AP-1 complex in cell-proliferation and transformation. *Biochim Biophys Acta* 1991;1072:129-57.

41. Beg AA, Baltimore D. An essential role for NF-kappaB in preventing TNF-alpha-induced cell death. *Science* 1996;274:782-4.

42. Van Antwerp DJ, Martin SJ, Kafri T, *et al*. Suppression of TNF-alpha-induced apoptosis by NF-kappaB. *Science* 1996;274:787-9.

43. Wang CY, Mayo MW, Baldwin AS Jr. TNF- and cancer therapy-induced apoptosis: potentiation by inhibition of NF-kappaB. *Science* 1996;274:784-7.

44. Hollander MC, Fornace AJ Jr. Induction of fos RNA by DNA-damaging agents. *Cancer Res* 1989; 49:1687-92.

45. Shaulian E, Karin M. AP-1 as a regulator of cell life and death. *Nature Cell Biol* 2002;4:E131-6.

46. Slater AF, Stefan C, Nobel I, *et al*. Intracellular redox changes during apoptosis. *Cell Death Differ* 1996;3:57-62.

47. Kluck RM, Bossy-Wetzel E, Green DR, Newmeyer DD. The release of cytochrome c from mitochondria: a primary site for Bcl-2 regulation of apoptosis. *Science* 1997;275:1132-6.

48. Kasinski AL, Du Y, Thomas SL, *et al*. Inhibition of IkappaB kinase-nuclear factor-kappaB signaling pathway by 3,5-bis(2-flurobenzylidene) piperidin-4-one (EF24), a novel monoketone analog of curcumin. *Mol Pharmacol* 2008; 74:654-61.

49. Brown A, Shi Q, Moore TW, *et al*. Monocarbonyl curcumin analogues: heterocyclic pleiotropic kinase inhibitors that mediate anticancer properties. *J Med Chem* 2013;56:3456 -66.

50. Landais I, Hiddingh S, McCarroll M, *et al*. Monoketone analogs (EF24) of curcumin, a new class of Fanconi anemia pathway inhibitors. *Mol Cancer* 2009;8:33- 45.

51. Thomas SL, Zhao J, Li Z, *et al*. Activation of the p38 pathway by a novel monoketone curcumin analog, EF24, suggests a potential combination strategy. *Biochem Pharmacol* 2010;80:1309-16.

52. Unruh D, Turner K, Srinivasan R, *et al*. Alternatively spliced tissue factor contributes to tumor spread and activation of coagulation in pancreatic ductal adenocarcinoma. *Int J Cancer* 2014; 134:9-20.

53. Chu Z, Abu-Baker S, Palascak MB, *et al*. Targeting and Cytotoxicity of SapC-DOPS Nanovesicles in Pancreatic Cancer. *PLOS One* 2013;8: e755507.

54. Shen Z, Peedikayil J, Olson GK, *et al*. Multiple transcription factor profiling by enzyme-linked immunoassay. *Biotechniques* 2002;32:1168,1170-2, 1174 passim.

55. Joshi AR, Chung CS, Son, *et al*. NF-kappa B activation has tissue specific effects on immune cell apoptosis during polymicrobial sepsis. *Shock* 2002; 18:380-6.

56. Benotmane AM, Hoylaerts MF, Colleen D, Belayew A. Nonisotopic quantitative analysis of protein-DNA interactions at equilibrium. *Anal Biochem* 1997;250:181-5.

57. Yates KR, Welsh J, Echrish HH, *et al*. Pancreatic cancer cell and microparticle procoagulant surface characterization: involvement of membrane-expressed tissue factor, phosphatidylserine and phosphatidylethanolamine. *Blood Coagul Fibrinolysis* 2011;22:680-7.

58. Haas SL, Jesnowski R, Steiner M, *et al*. Expression of tissue factor in pancreatic adenocarcinoma is associated with activation of coagulation. *World J Gastroenterol* 2006;12:4843-9.

59. Ran S, He J, Huang X, *et al*. Antitumor effects of a monoclonal antibody that binds anionic phospholipids on the surface of tumor blood vessels in mice. *Clin Cancer Res* 2005;11:1551-62.

60. Kocatürk B, Van den Berg YW, Tieken C, *et al*. Alternatively spliced tissue factor promotes breast cancer growth in a β1 integrin-dependent manner. *Proc Natl Acad Sci U S A* 2013;110:11517-22.

61. van den Berg YW, Osanto S, Reitsma PH, Versteeg HH. The relationship between tissue factor and cancer progression: insights from bench and bedside. *Blood* 2012;119:924-32.

62. Kaushal V, Mukunyadzi P, Siegel ER, *et al*. Expression of tissue factor in prostate cancer correlates with malignant phenotype. *Appl Immunohistochem Mol Morphol* 2008;16:1-6.

63. Jobin C, Bradham CA, Russo MP, *et al*. Curcumin blocks cytokine-mediated NF-kappa B activation and proinflammatory gene expression by inhibiting inhibitory factor I-kappa B kinase activity. *J Immunol* 1999;163:3474-83.

64. Bergelson S, Pinkus R, Daniel V. Induction of AP-1 (Fos/Jun) by chemical agents mediates activation of glutathione S-transferase and quinone reductase gene expression. *Oncogene* 1994;9:565-71.

65. Hartsfield CL, Alam J, Choi AM. Transcriptional regulation of the heme oxygenase 1 gene by pyr-

rolidine dithiocarbamate. *FASEB J* 1998;**12**:1675-82.

66. Yen FL, Tsai MH, Yang CM, et al. Curcumin nanoparticles ameliorate ICAM-1 expression in TNF-α-treated lung epithelial cells through p47 (phox) and MAPKs/AP-1 pathways. *PLoS One* 2013;**8**:e63845.

67. Jeschke J, O'Hagan HM, Zhang W, *et al*. Frequent inactivation of cysteine dioxygenase type 1 contributes to survival of breast cancer cells and resistance to anthracyclines. *Clin Cancer Res* 2013;**19**:3201-11.

68. Musselman CA, Kutateladze TG. PHD fingers: epigenetic effectors and potential drug targets. *Mol Interv* 2009;**9**:314-23.

69. Malik P, Mukherjee TK. Structure-Function Elucidation of Antioxidative and prooxidative Activities of the Polyphenolic Compound Curcumin. *Chinese J Biol* 2014;**2014**:396708.

70. Tang NY, Huang YT, Yu CS, *et al*. Phenethyl isothiocyanate (PEITC) promotes G2/M phase arrest via p53 expression and induces apoptosis through caspase- and mitochondria-dependent signaling pathways in human prostate cancer DU 145 cells. *Anticancer Res* 2011;31:1691-702.

71. Owuor ED, Kong A-NT. Antioxidants and oxidants regulated signal transduction pathways. *Biochem Pharmacol* 2002;**64**:765-70.

72. Baglole CJ, Sime PJ, Phipps RP. Cigarette smoke-induced expression of heme oxygenase-1 in human lung fibroblasts is regulated by intracellular glutathione. *Am J Physiol Lung Cell Mol Physiol* 2008;**295**:L624-36.

73. Kong AN, Yu R, Lei W, *et al*. Differential activation of MAPK and ICE/Ced-3 protease in chemical-induced apoptosis: The role of oxidative stress in the regulation of mitogen-activated protein kinases (MAPKs) leading to gene expression and survival or activation of caspases leading to apoptosis. *Restor Neurol Neurosci* 1998;**12**:63-70.